Coupled ocean-atmosphere interactions and local impact of mesoscale SST on atmospheric boundary layer in the Kuroshio region (M164A)

Dian Putrasahan (dputrasa@ucsd.edu), Art Miller (ajmiller@ucsd.edu), Scripps Institution of Oceanography, UCSD
Hyodae Seo (hseo@whoi.edu), Woods-Hole Oceanographic Institution

Introduction

The Kuroshio region has pronounced oceanic currents and SST fronts that consequently impacts the atmosphere. Using a regional coupled model and satellite observations, we set up an experiment to quantify air-sea coupling that includes the mesoscale, as well as to investigate the consequences of removing the mesoscale eddy influence on the ABL while maintaining the large-scale SST coupling. This study attempts to address the following questions:

- How much impact does mesoscale SST have on the overlying PBL structure and precipitation of this region?
- How does the SST distribution affect the sensible and latent heat fluxes over the Kuroshio region?
- What is the seasonal variability of the air-sea feedbacks in the Kuroshio region? Particularly, through which mechanism and at what scale does SST influence the atmospheric dynamics of the region?

Mesoscale SST Experiment	
Case 1: (Control)	Control run composed of fully-coupled SCOAR run for 2000-2007
Case 2: (Smoothed)	SCOAR run with daily, 3 degrees spatial smoothing of SST at every coupling step

Model and Satellite Observations

We employed the Scripps Coupled Ocean-Atmosphere Regional (SCOAR) model to perform air-sea interaction studies in this region. The model consists of the Experimental Climate Prediction Center (ECPC) Regional Spectral Model (RSM) as the atmospheric component, the Regional Ocean Modeling System (ROMS) as the oceanic part, and a flux-SST coupler built by Seo et al. (2007a) to bridge the two. In addition, we have implemented an online, 2-D, spatial SST smoother at each coupling step to simulate large-scale coupling.

Model Specifications	
Domain	125E-165E, 31N-47N
Grid Resolution & Boundary Conditions	Horizontal: 25km Ocean: 30 layers (OFES monthly) Atmos.: 28 layers (NCEP R2 daily)
Time Period	Jan 2000 – Dec 2007

Satellite observations were used to study ocean-atmosphere phenomenon, as well as to validate model output. Below is a table of satellite products utilized in this study.

Variable	Observations	Frequency	Resolution
SST	TMI-AMSRE	Daily	$0.25^o \times 0.25^o$
Wind stress	QuikSCAT	Daily	$0.5^o \times 0.5^o$
Surface Heat Fluxes	OA Flux	Monthly	$1^o \times 1^o$

1. SST and ABL

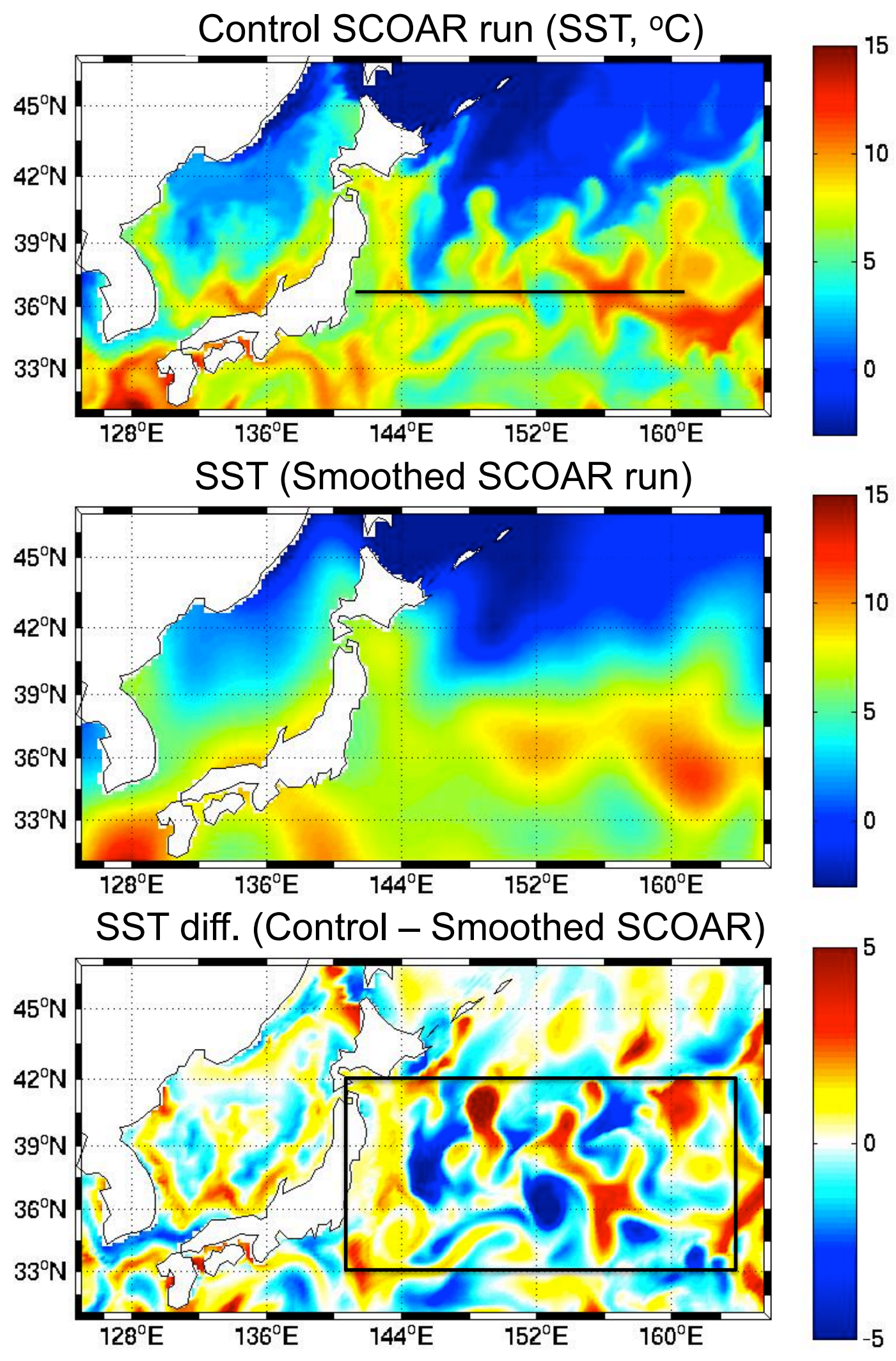

Figure 1 (above): Monthly averaged SST distribution for Control SCOAR (top), Smoothed SCOAR (middle) and difference between control and smoothed SCOAR (bottom)

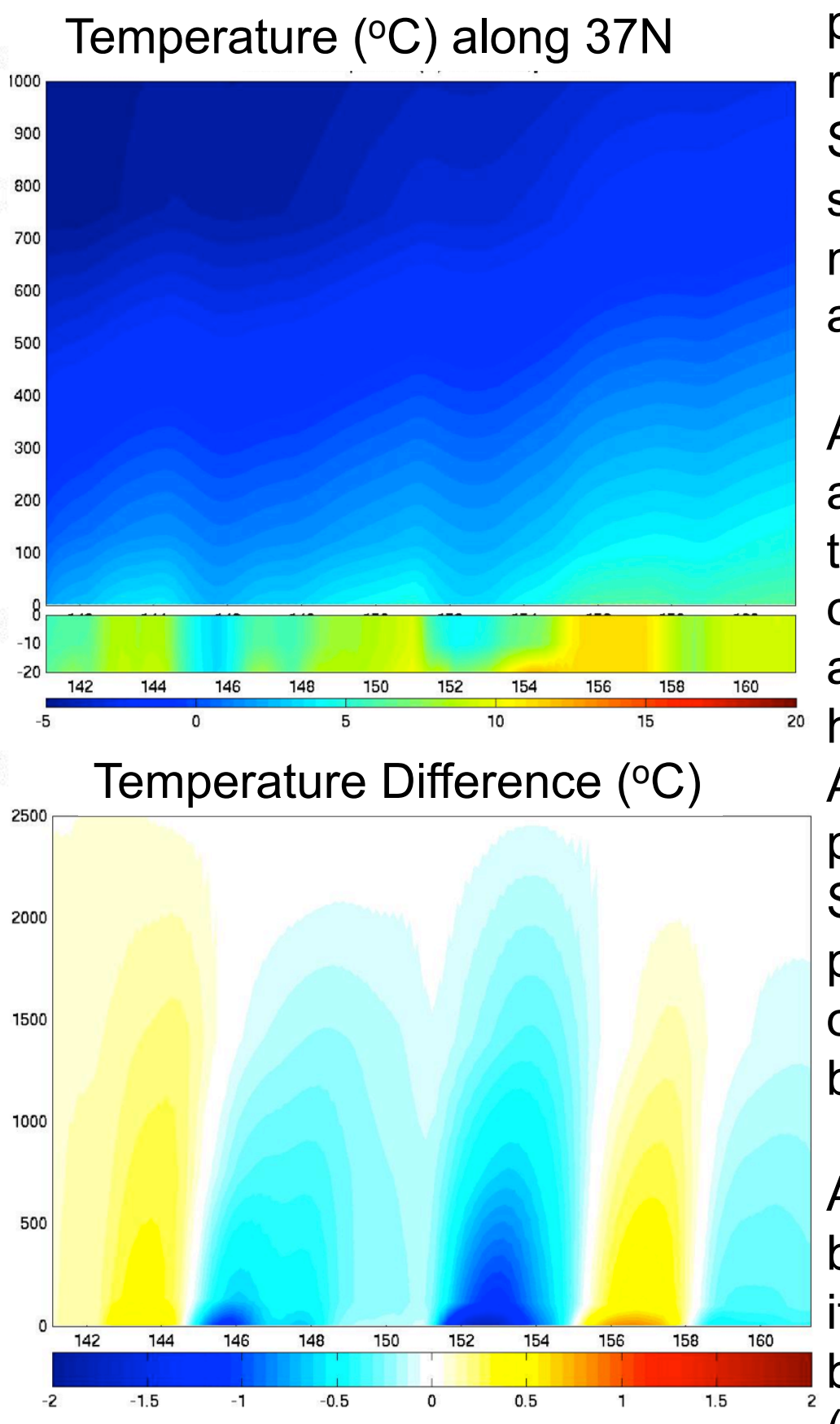

Figure 2 (above): (a) Vertical cross section of the ocean and the atmospheric temperature at 37N latitude; (b) vertical atmospheric temperature difference between control and smoothed SCOAR

ROMS was able to freely evolve and produce mesoscale features as reflected on the SST map of the control SCOAR run (Fig.1, top). The 2-D spatial smoother effectively filtered out mesoscale features of up to 3 degrees, as seen in the middle map of Fig. 1.

A vertical temperature cross section along 37N latitude of the surface ocean to the atmosphere shows that the oceanic mesoscale imprint on the atmosphere can reach significant heights (Fig. 2, top).

A difference in the vertical temperature profile between control and smoothed SCOAR run provides insights to the penetration depth (~2000m) of these oceanic mesoscale features (Fig. 2, bottom).

A region of significant SST differences between the 2 runs was chosen to study its affect of the ABL (boxed area in bottom Fig. 1). The difference maps (Fig. 3) illustrate how surface heat flux and PBL height co-vary very well with different SSTs. There is a slight shift in precipitation with respect to peak SST difference, however, precipitation co-locates closely with wind convergence.

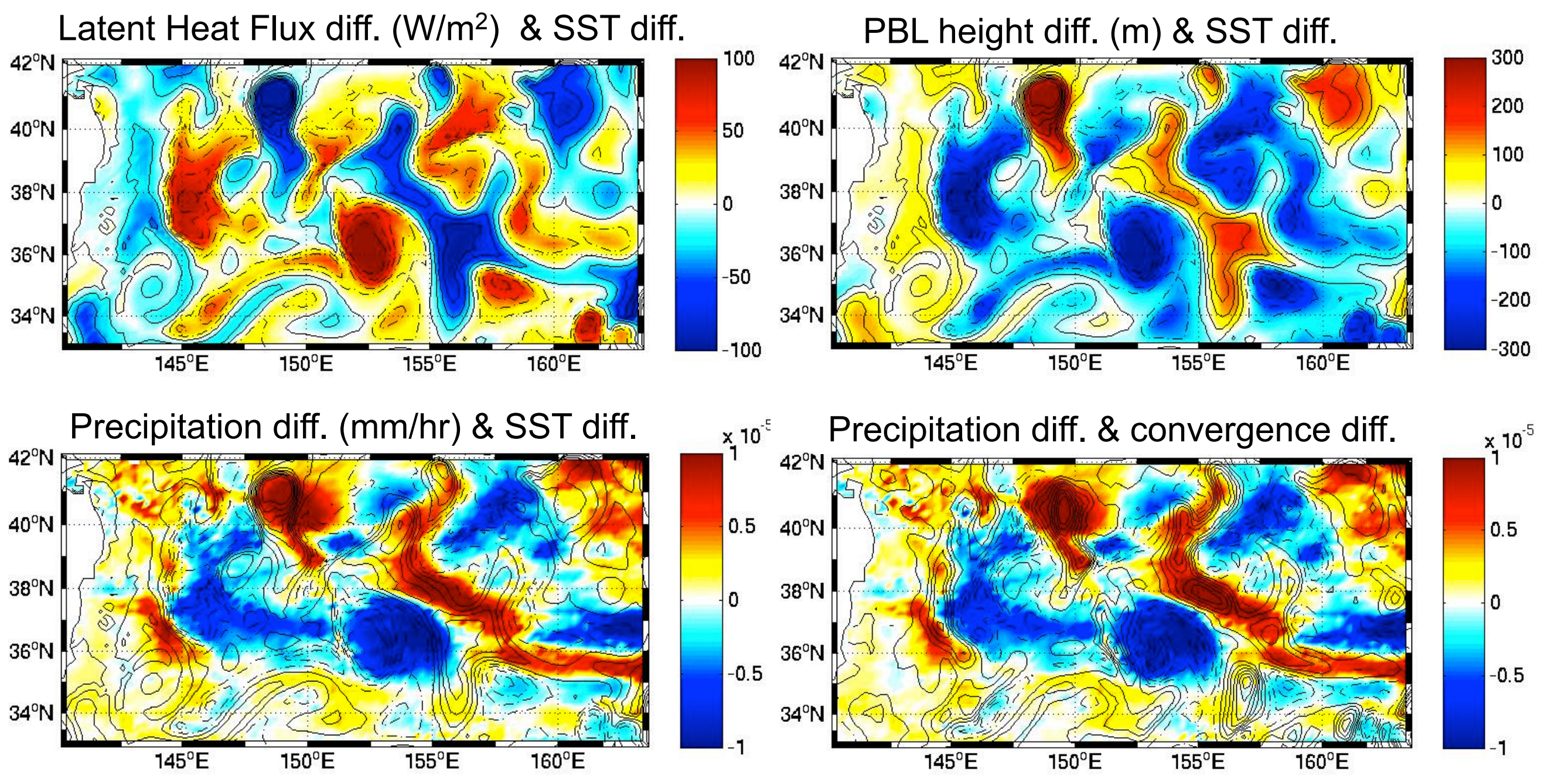

Figure 3 (right): Color maps of differences in (a) latent heat flux; (b) PBL height; (c)&(d) precipitation between control and smoothed SCOAR. (a-c) are overlaid with contours of SST differences, while (d) is overlaid with contours of differences in 10m wind convergence

2. SST and surface heat flux

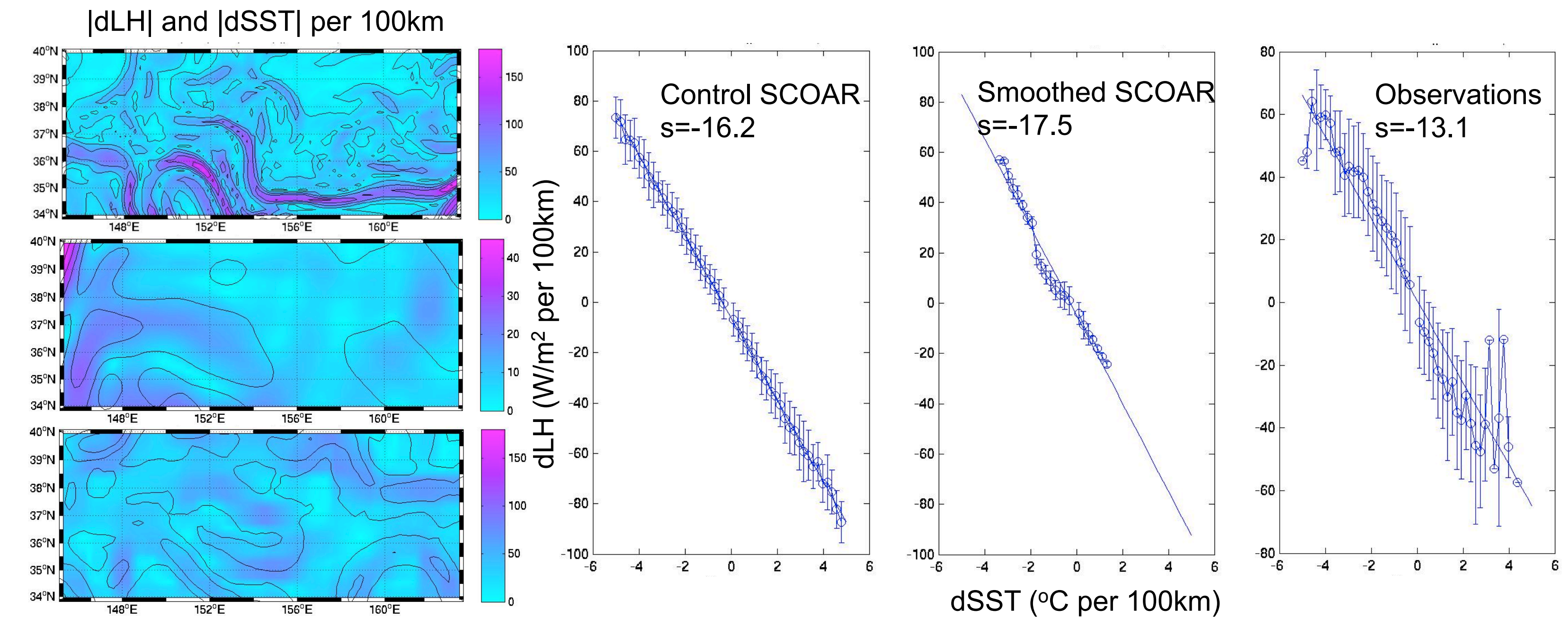

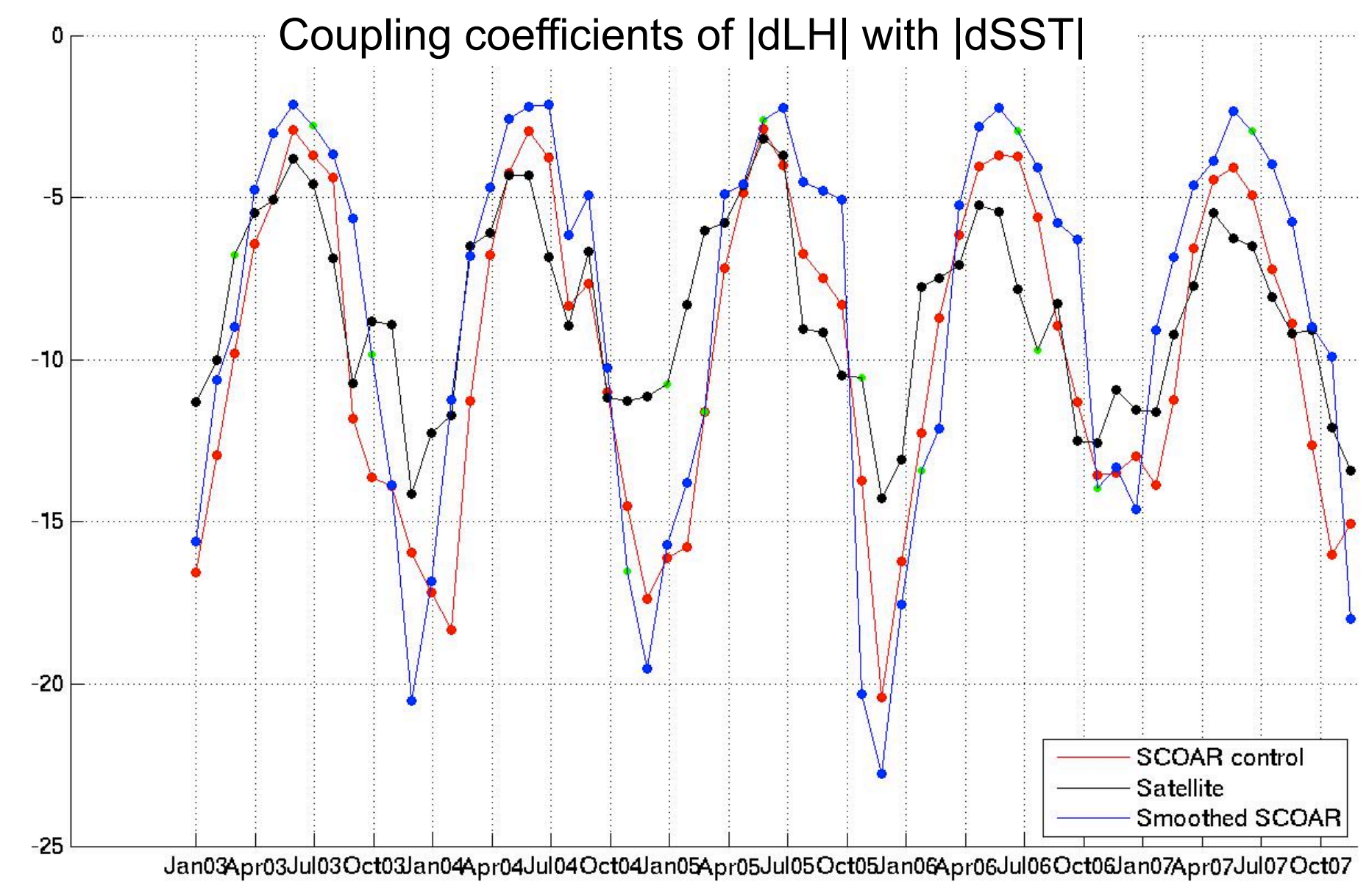

Figure 4 (above): Left panel has color maps of spatial derivatives of latent heat flux overlaid with contours of SST spatial derivatives over the region (34N-40N, 145E-163E), averaged during January 2006, for control SCOAR (top), smoothed SCOAR (middle) and observations (bottom). Subsequent panels are linear fits of the bin-scatter plots of corresponding variables, and their coupling coefficients (s). Error bars are one standard deviation from the mean of each bin.

Figure 5 (left): Time series of monthly coupling coefficients of latent heat flux gradient with SST gradient for the period of 2003-2007. Red (control SCOAR), black (observations) and blue (smoothed SCOAR) dots indicate values that have r^2 significance greater than 0.9, while green dots indicate otherwise.

Latent heat flux out of the ocean is affected by SST both directly, by altering the stability of the ABL and indirectly by the influence of SST on the wind speed variations. Increased winds over warmer waters enhances evaporative cooling, thus decreasing SST (negative feedback). A negative linear relationship between changes in latent heat flux with changes in SST is seen in Figure 4. Although the control SCOAR has stronger SST gradients than the smoothed SCOAR, the coupling coefficient are alike, suggesting similar contribution of large-scale and mesoscale coupling to the surface heat flux-SST coupling.

There is a clear seasonal cycle to the coupling, with its peak in winter (Figure 5). Similar results were obtained for sensible heat flux (not shown).

3. SST and Wind Stress

There are two well-known mechanisms that explain the response of wind in SST frontal regions, namely the vertical mixing mechanism and the pressure adjustment mechanism. The vertical mixing mechanism suggests that warmer (colder) SST reduces (enhances) the stability of the overlying atmosphere, which supports (inhibits) the downward transfer of momentum through mixing, that would thus increase (decrease) surface winds (Wallace et. al, 1989). When this occurs over an SST gradient, it can lead to wind stress divergence and curl at the surface (Chelton et. al, 2001).

Over an active mesoscale eddy region, the control run, smoothed run and observations show comparable coupling between wind stress divergence and downwind SST gradients (Fig. 6). Note that even though the strength of the downwind SST gradients for the control and smoothed SCOAR runs are different, the coupling coefficients (slope of the linear fit, s) are comparable. This suggests that the air-sea coupling through this mechanism occurs on both large-scale and mesoscale, at similar magnitudes. This particular air-sea coupling has a seasonal cycle and is pronounced and significant during the winter season (Fig. 7).

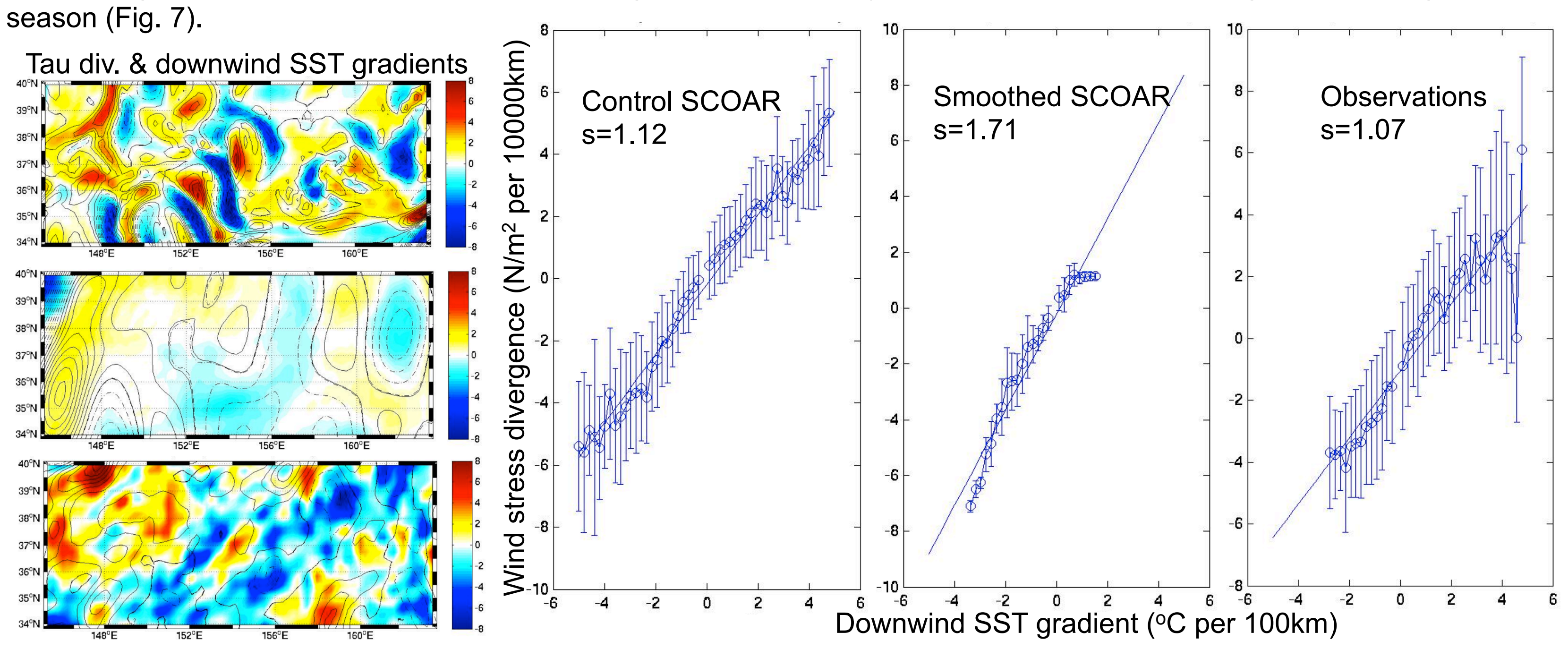

Figure 6 (above): Left panel: Color maps of wind stress divergence overlaid with contours of downwind SST gradients over the region (34N-40N, 145E-163E), averaged during January 2006, for control SCOAR (top), smoothed SCOAR (middle) and observations (bottom). For better quantification, linear fit was performed on bin-scatter plots of aforementioned variables, and shown on following panels, along with their coupling coefficients (s). Error bars are one standard deviation from the mean of each bin.

Figure 7 (below, left): Time series of monthly coupling coefficients of wind stress divergence and downwind SST gradient for the period of 2003-2007. Red (control SCOAR), black (observations) and blue (smoothed SCOAR) dots indicate values that have r^2 significance greater than 0.85, while green dots indicate otherwise.

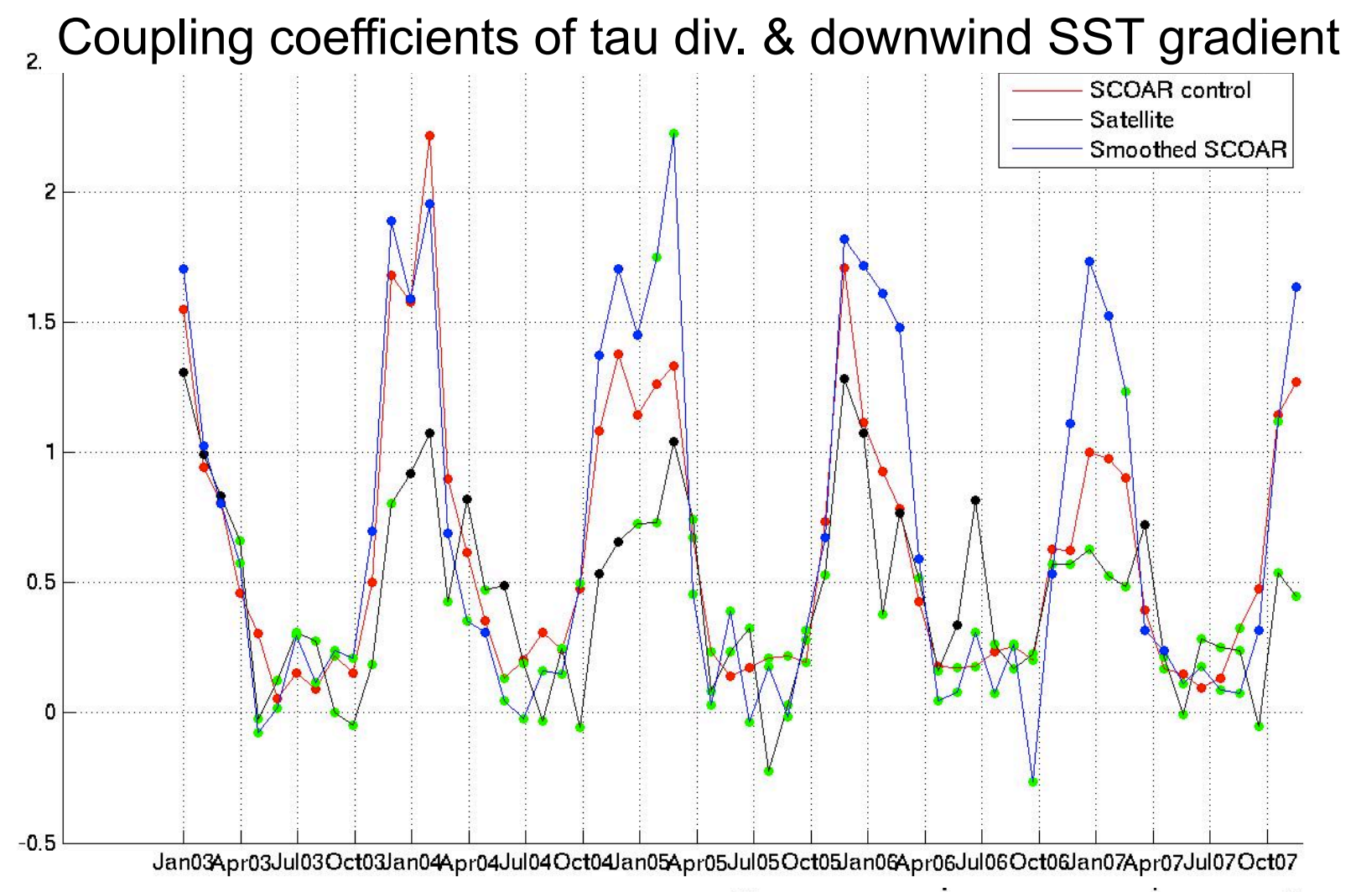

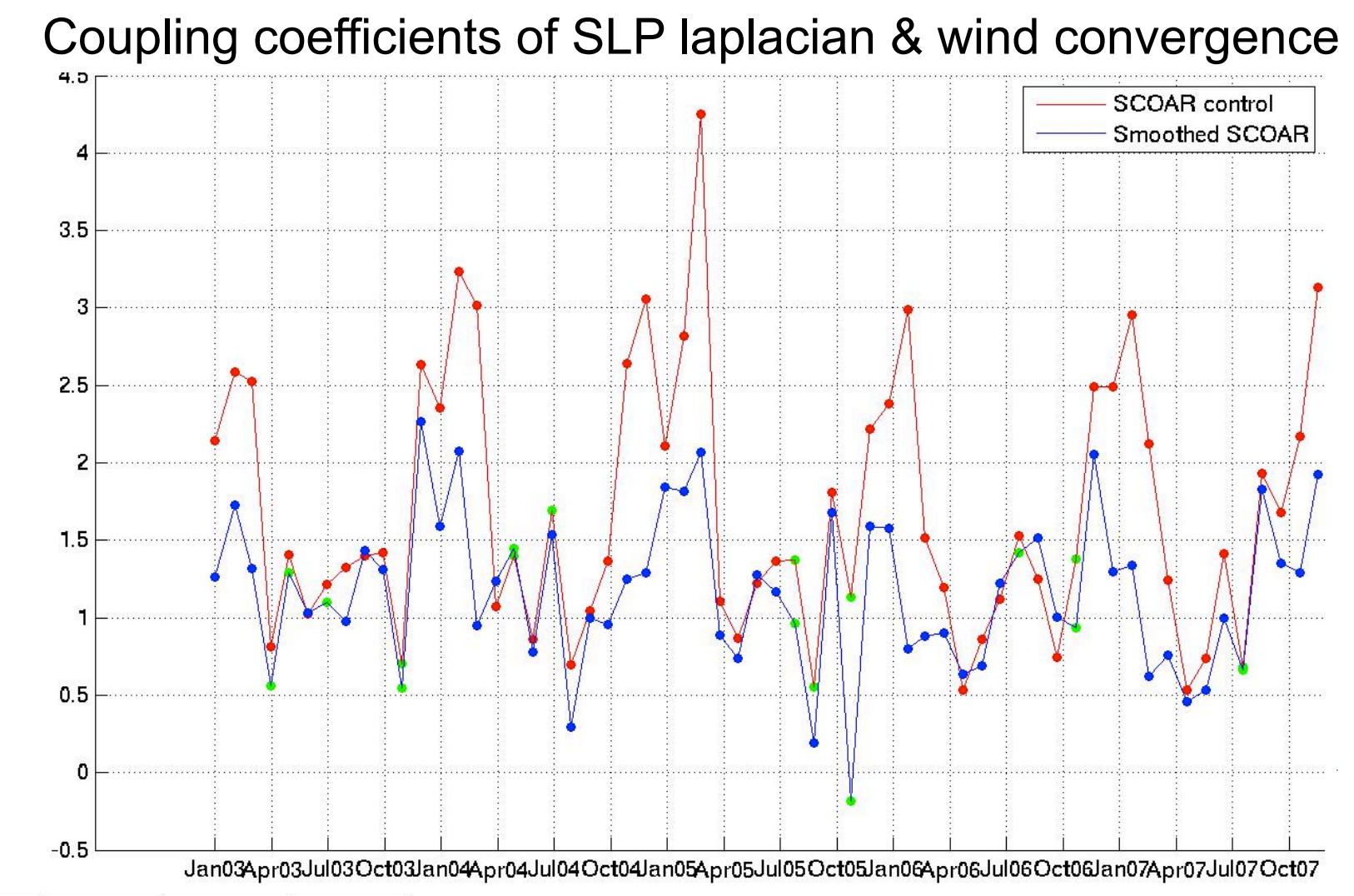

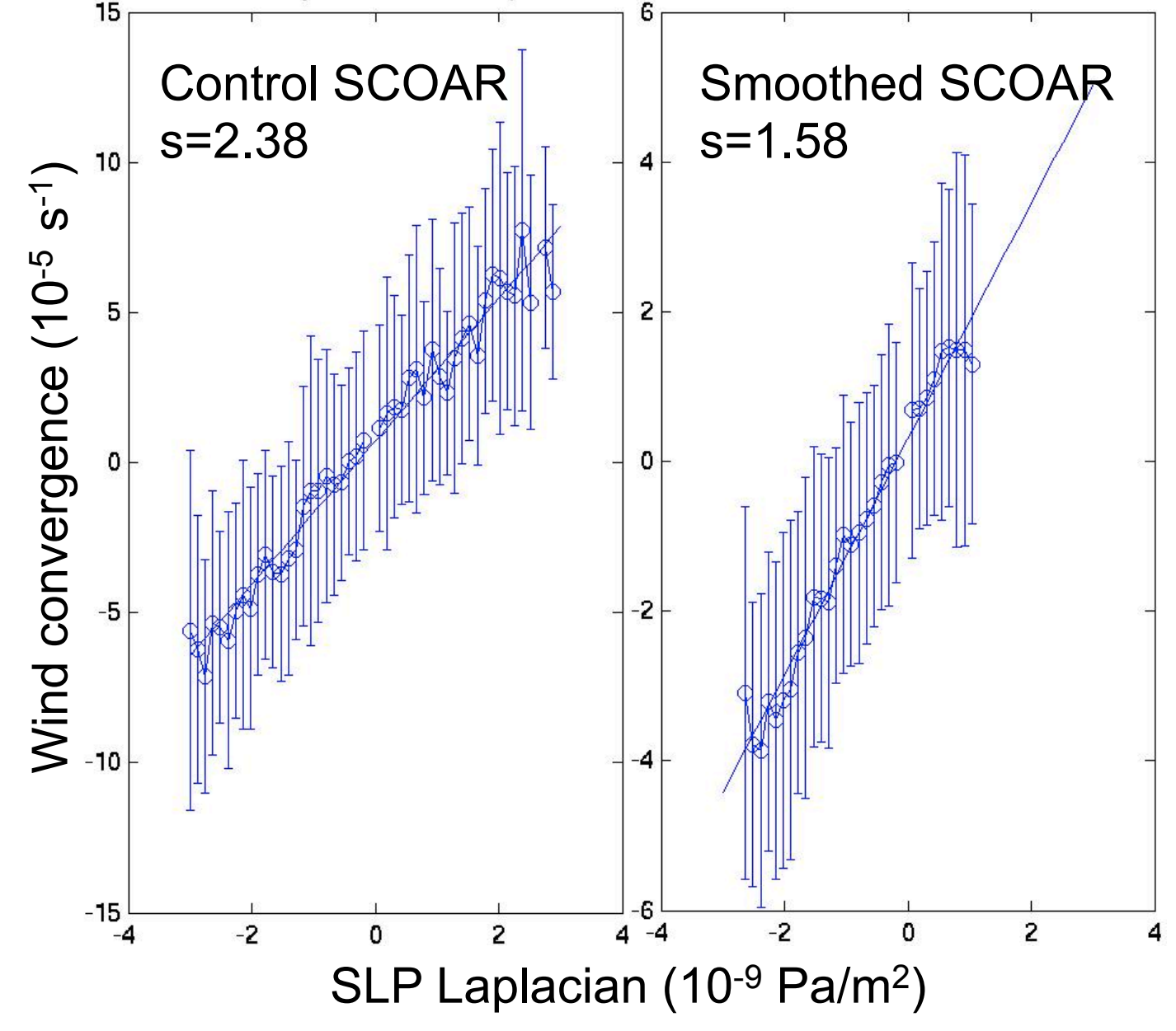

Figure 8 (above): Linear fits to bin-scatter plot of 10m wind convergence against SLP laplacian over the region (34N-40N, 145E-163E), averaged during January 2006, for control SCOAR ((left) and smoothed SCOAR (right). Coupling coefficients (s) were computed and error bars are one standard deviation from the mean of each bin.

Figure 9 (above, right): Time series of monthly coupling coefficients of SLP laplacian with 10m wind convergence for the period of 2003-2007. Red (control SCOAR), black (observations) and blue (smoothed SCOAR) dots indicate values that have r^2 significance greater than 0.85, while green dots indicate otherwise.

The pressure adjustment mechanism (Lindzen and Nigam, 1989) suggests that warm (cold) SST anomalies induces low (high) surface pressure anomalies that would promote convergence (divergence) of surface winds. This is reflected in the linear relationship of wind convergence and SLP laplacian.

Both control SCOAR and smoothed SCOAR indicate such relationship exist (Fig. 8), and that there is also a seasonal cycle, with peak coupling in winter seasons (Fig. 9).

Reference

➢D. Putrasahan, A. Miller, and H. Seo. Local impact of mesoscale SST on atmospheric boundary layer and coupled ocean-atmosphere interactions in the Kuroshio region. 2011 in prep.

➢H. Seo, A. Miller, and J. Roads. The Scripps Coupled Ocean-Atmosphere Regional (SCOAR) model, with applications in the eastern Pacific sector. *Journal of Climate*, 20:381–402, 2007.

➢D. Chelton, S. Esbensen, M. Schlax, N. Thum, M. Freilich, F. Wentz, C.L.Gentemann, M. McPhaden, and P. Schopf. Observations of coupling between surface wind stress and sea surface temperature in the eastern tropical Pacific. *Journal of Climate*, 14:1479–1498, 2001.

➢J. Wallace, T. Mitchell, and C. Deser. The influence of sea surface temperature on surface wind in the eastern equatorial Pacific: seasonal and interannual variability. *Journal of Climate*, 2:1492–1499, 1989.

➢R. Lindzen, and S. Nigam. On the role of sea surface temperature gradients in forcing low-level winds and convergence in the tropics. *Journal of Atmospheric Sciences*, 44:2418-2436, 1987.